Dynamical evolution of boson stars in Brans-Dicke theory

Jayashree Balakrishna* and Hisa-aki Shinkai†
Department of Physics, Washington University, St. Louis, Missouri 63130-4899
(Received 13 November 1997; published 23 July 1998)

We study the dynamics of a self-gravitating scalar field solitonic object (boson star) in the Jordan-Brans-Dicke (BD) theory of gravity. We show dynamical processes of this system such as (i) black hole formation of a perturbed equilibrium configuration on an unstable branch, (ii) migration of a perturbed equilibrium configuration from an unstable branch to a stable branch, and (iii) the transition from an excited state to a ground state. We find that the dynamical behavior of boson stars in BD theory is quite similar to that in general relativity (GR), with comparable scalar wave emission. We also demonstrate the formation of a stable boson star from a Gaussian scalar field packet with flat gravitational scalar field initial data. This suggests that boson stars can be formed in the BD theory in much the same way as in GR. [S0556-2821(98)00916-3]

PACS number(s): 04.40.Dg, 04.50.+h

I. INTRODUCTION

Gravitational solitonic objects are quite an interesting topic in general relativity (GR). A boson star consists of a massive complex scalar field, and was first discussed by Kaup [1] and then by Ruffini and Bonazzola [2] (for a thorough review, see [3,4]). They can form stable configurations having negative binding energy, as a result of a balance of the dispersion due to the classical analogue of the uncertainty principle and the attractive effects of gravity. If we include even a small self-interaction term, then their maximum allowed stable mass can be close to the order of a solar mass [5]. It is also speculated that they are a form of dark matter that could have been created during a phase transition in the early universe (see Frieman *et al.* [6]). Although we still have no evidence for their astrophysical existence, these systems are a good model from which to learn the nature of a strong gravitational field.

The stability of boson stars has also been studied by several authors. Lee and Pang [7] discussed ground state stability using linearized perturbation theory, and Seidel and Suen [8] studied their dynamical behavior by evolving field equations numerically. In GR, the ground state boson star configurations are comprised of a stable branch and an unstable branch. Upon perturbations, boson stars on the stable branch remain on the stable branch, settling down into a configuration with a different mass. In the process, it emits scalar radiation with some characteristic normal mode frequencies. On the other hand, stars on the unstable branch do not remain there after perturbations. They either disperse completely, form black holes, or migrate to the stable branch depending on the size of the perturbations. These qualitative features are also discussed applying catastrophe theory [9]. Recently, Balakrishna, Seidel, and Suen [10] studied dynamical boson stars with the self-coupling term and excited states. They found that excited state boson star equilibrium configurations have branches similar to that of the ground state, but all branches are unstable.

In this paper, we study the dynamical behavior of boson stars in the Jordan-Brans-Dicke (BD) theory of gravity [11]. In particular, we compare the dynamics with those in GR. The BD theory is one of the alternative theories of gravity to GR, and the most simple and prototype in all the scalar-tensor theories of gravity (see Will [12] for a review). The previous experimental test using the delay of radar echos in the solar system shows the bound of the BD parameter as $\omega_{\rm BD}>500$ [13,14], of which the infinite limit agrees with GR. This bound is also considered to be limited by the direct observations of gravitational waves (see [15] and references therein). (Recently, more strict limitations of the BD parameter $\omega_{\rm BD}$ are reported [16]: however, the results are model dependent and we think $\omega_{\rm BD}>500$ is still the generally accepted observational limit.)

So far, boson stars in scalar-tensor gravity have also been discussed by Gundersen and Jensen [17] and Torres [18] who showed the existence of equilibrium ground state boson star solutions in the BD coupling and in the three different couplings in the scalar-tensor theories, respectively. Comer and Shinkai [19] showed the existence of excited state boson stars in both BD and the Damour-Nordtvedt quadratic coupling (attractor) model [20] in the scalar-tensor theories. They also discussed the stabilities of ground state boson stars using catastrophe theory. One of our purposes of this paper is to study the stability of boson stars in BD theory. By evolving the field equations numerically for slightly or heavily perturbed equilibrium data, we clarify the stability of boson stars both for ground and excited states.

Our system includes two scalar fields: the bosonic matter (complex and massive) scalar field and the gravitational (real and massless) scalar field (which hereafter we call the BD field). We expect to be able to study the fundamental mechanism of the interactions between these two fields in their dynamics. Several previous simulations have shown emissions of scalar waves in BD [21–23] or scalar-tensor theory [24,25] from a collapse of the dust or star model. Our second interest is in how much difference appears in the scalar gravitational wave emissions during the dynamical boson star system between BD theory and GR: whether they will be enhanced or suppressed.

Throughout this paper, we stand at the point to see if they

*Email: bala@wurel.wustl.edu
†Email: shinkai@wurel.wustl.edu

in any way differ from boson stars in a detectable manner; that is, we impose $\omega_{\rm BD} > 500$ in most simulations.

The outline of this paper is as follows. In Sec. II, we will introduce the field equations and basic outline of our numerical techniques. With a view to study this problem in scalar-tensor theories in the near future [32], we describe fundamental equations not only in BD theory but in general scalar-tensor theories.

We describe the equilibrium configuration briefly in Sec. III. We plot the sequences of excited state configurations in BD theory and also discuss fractional anisotropy measurements in this system, both of which have not appeared before in the references.

Section IV is devoted to stable boson star configurations. In GR, under the effects of finite perturbations, these stars react by expanding and contracting with emitting scalar radiation at each expansion [8]. The star loses mass and settles to a lower mass configuration. Each expansion (contraction) of the core of the star is accompanied by the contraction (expansion) of the radial metric. We study whether the expansions and contractions of the star set the BD field into oscillations and whether this results in any measurable gravitational radiation in addition to the scalar radiation. Under infinitesimal perturbations, boson stars in GR start oscillating at their fundamental quasinormal mode frequencies that remain constant and virtually undamped for large periods of time. We also study whether this is seen in BD theory.

Section V shows the behavior of unstable boson stars. In GR, equilibrium boson stars on the unstable branch, when perturbed, begin forming black holes or migrating to a new equilibrium configuration on the stable branch. The excited state configurations of boson stars are expected to be unstable. If they cannot lose enough mass and settle to the ground state configuration, they collapse to black holes. We also show the cascading of a BD boson star in an excited state to the ground state.

In Sec. VI, we look at the formation of boson stars in BD theory. The collection of bosonic matter localized in a region of space is represented by a Gaussian initial boson field. The BD field itself is initially set to zero: we discuss whether or how an equilibrium configuration actually forms in BD theory. Finally, in Sec. VII we make some concluding remarks.

We use the units $c=1$ and $\hbar=1$. This implies that the scalar field mass m is an inverse length (actually, the inverse Compton wavelength of the scalar particles) and the bare gravitational constant G_* has units of length squared.

II. FIELD EQUATIONS

In this section, we present our basic field equations, boundary conditions, and numerical techniques to solve the system. For our future convenience [32], we show the field equations not only in the Brans-Dicke theory of gravity ($\omega = \omega_{\rm BD} = \text{const}$), but also in the general scalar-tensor theory of gravity [$\omega = \omega(\phi)$].

A. Lagrangians and field equations

The action for our system of scalar-tensor gravity coupled to a self-interacting, complex scalar field in the physical ''Jordan frame'' is

$$S_J = \frac{1}{16\pi}\int d^4x\sqrt{-\tilde{g}}\,[\phi\tilde{R} - \phi^{-1}\omega(\phi)\tilde{g}^{\mu\nu}\partial_\mu\phi\partial_\nu\phi] - \int {\rm d}^4x\sqrt{-\tilde{g}}\left[\frac{1}{2}\,\tilde{g}^{\mu\nu}\partial_\mu\psi^\dagger\partial_\nu\psi + V(\psi^\dagger\psi)\right]. \tag{2.1}$$

The gravitational scalar is ϕ and $\omega(\phi)$ is the Jordan-frame coupling of ϕ to the matter. The complex scalar ψ (with its complex conjugate being $\psi^\dagger$) has mass m and is self-interacting through the potential

$$V(\psi^\dagger\psi) = \frac{m^2}{2}\,\psi^\dagger\psi + \frac{\Lambda}{4}\,(\psi^\dagger\psi)^2. \tag{2.2}$$

The strength of the self-interaction, Λ, is normally taken to be positive.

There is an alternative representation of the action above, the so-called ''Einstein frame.'' The expression is given by the conformal transformation

$$\tilde{g}_{\mu\nu} = e^{2a(\varphi)}g_{\mu\nu}, \tag{2.3}$$

where $a(\varphi)$ is the functional transformation from ϕ to the Einstein-frame gravitational scalar φ,

$$\phi^{-1} = G_* e^{2a(\varphi)}, \tag{2.4}$$

where G_* is the effective gravitational constant in the Einstein frame. The relationship between $\omega(\phi)$ and $a(\varphi)$ is obtained from

$$\alpha^2 = (2\omega+3)^{-1}, \tag{2.5}$$

where

$$\alpha(\varphi) \equiv \frac{\partial a}{\partial\varphi}. \tag{2.6}$$

The action in the Einstein frame is thus

$$S_E = \frac{1}{16\pi G_*}\int {\rm d}^4x\sqrt{-g}\,[R - 2g^{\mu\nu}\partial_\mu\varphi\partial_\nu\varphi] - \int {\rm d}^4x\sqrt{-g}\left[\frac{1}{2}\,e^{2a(\varphi)}g^{\mu\nu}\partial_\mu\psi^\dagger\partial_\nu\psi + e^{4a(\varphi)}V(\psi^\dagger\psi)\right]. \tag{2.7}$$

It does not deliver GR exactly because the metric $g_{\mu\nu}$ is not the true physical metric that encodes the distance between spacetime points. However, the Einstein frame does deliver equations that are similar enough to GR that we will use it for our calculations.

The Einstein-frame stress-energy tensor is

$$T_{\mu\nu} = \frac{1}{2}e^{2a(\varphi)}(\partial_\mu\psi^\dagger\partial_\nu\psi + \partial_\nu\psi^\dagger\partial_\mu\psi) - \frac{1}{2}\,e^{2a(\varphi)}[\partial_\tau\psi^\dagger\partial^\tau\psi + 2e^{2a(\varphi)}V(\psi^\dagger\psi)]g_{\mu\nu}. \tag{2.8}$$

The gravitational field equations for $g_{\mu\nu}$ and φ are

$$G_{\mu\nu}=8\pi G_* T_{\mu\nu}+2\partial_\mu\varphi\partial_\nu\varphi-\partial_\tau\varphi\partial^\tau\varphi g_{\mu\nu} \tag{2.9}$$

and

$$\nabla_\sigma\nabla^\sigma\varphi=-4\pi\alpha T, \tag{2.10}$$

where T is the trace of the stress-energy tensor. The matter field equations are

$$\nabla_\sigma\nabla^\sigma\psi^\dagger+2\alpha\partial_\tau\psi^\dagger\partial^\tau\varphi=2e^{2a(\varphi)}\frac{\partial V}{\partial\psi}, \tag{2.11}$$

$$\nabla_\sigma\nabla^\sigma\psi+2\alpha\partial_\tau\psi\partial^\tau\varphi=2e^{2a(\varphi)}\frac{\partial V}{\partial\psi^\dagger}. \tag{2.12}$$

The coupling function $a(\varphi)$ is given by choosing a theory of gravity. In this paper, we only consider the Brans-Dicke coupling

$$a(\varphi)=\frac{\varphi-\varphi_\infty}{\sqrt{2\omega_{BD}+3}}, \tag{2.13}$$

where the parameter $\omega=\omega_{\rm BD}$ is constant, which observational constraint is known as $\omega_{\rm BD}>500$ [13,14]. The term φ_∞ represents the asymptotic value of the gravitational scalar field.

Because the potential $V(\psi^\dagger\psi)$ is a functional of $\psi^\dagger\psi$, it preserves the global U(1) gauge symmetry ($\psi\rightarrow e^{i\sigma}\psi$, where σ is a constant) present in the theory. This symmetry results in a conserved current, whose explicit form in the Jordan frame is

$$\tilde{J}^\mu=\frac{i}{2}e^{-2a(\varphi)}g^{\mu\nu}(\psi\partial_\nu\psi^\dagger-\psi^\dagger\partial_\nu\psi). \tag{2.14}$$

This conserved current leads to a conserved charge, which is N_p, the number of particles making up the star:

$$N_p=\int d^3x\sqrt{-g}\tilde{J}^t. \tag{2.15}$$

The spacetime considered here is spherically symmetric, with the Einstein-frame metric taking the form

$$ds^2=-N^2(t,r)dt^2+g^2(t,r)dr^2+r^2[d\theta^2+\sin^2\theta d\phi^2], \tag{2.16}$$

where N is the lapse function and r is the circumferential radius. We dropped the shift vector, since we use a polar-slicing condition [26] in evolution.

In this coordinate system, the Jordan-frame Arnowitt-Deser-Misner (ADM) mass M_J is given by

$$G_* M_J=\lim_{r\rightarrow\infty}\frac{r}{2}(1-1/\tilde{g}_{rr}). \tag{2.17}$$

The similar Einstein-frame ADM mass M_E is

$$G_* M_E=\lim_{r\rightarrow\infty}\frac{r}{2}(1-1/g_{rr}). \tag{2.18}$$

However, since $\tilde{g}_{rr}=e^{2a(\varphi)}g_{rr}$ and we set $a(\varphi_\infty)=0$ (to be discussed below), then the limits on the right-hand sides are equal and therefore $M_J=M_E\equiv M$.

B. Equilibrium state equations

The gravitational scalar, which is real, is assumed also to be spherically symmetric and static when we solve the equilibrium configuration:

$$\varphi=\varphi(r). \tag{2.19}$$

As for the matter scalar field, Friedberg *et al.* [27] show that the minimum energy configurations are those for which

$$\psi=e^{-i\Omega t}\Phi(r), \tag{2.20}$$

where Ω is real and positive and $\Phi(r)$ is real function. Their proof (see the Appendix in [27]) also goes through for scalar-tensor gravity, and so we will take ψ to have this form.

We will take advantage of the scale invariance of the field equations to redefine some of the fields, parameters, and the radial and time coordinates:

$$mr\rightarrow r,\quad \sqrt{4\pi G_*}\Phi\rightarrow\Phi,\quad mN/\Omega\rightarrow N,$$
$$\Lambda/4\pi G_* m^2\rightarrow\Lambda,\quad \Omega t/m\rightarrow t. \tag{2.21}$$

Note that the rescaling changes the asymptotic value of N, which is now

$$\lim_{r\rightarrow\infty}N(x)=m/\Omega. \tag{2.22}$$

The field equations, then, become

$$\partial_r\partial_r\varphi=\left[-\frac{g^2+1}{r}+2e^{4a}rg^2V(\Phi)\right]\partial_r\varphi + g^2\left\{2\alpha e^{2a}\left[\frac{1}{2}\nabla_\sigma\Phi\nabla^\sigma\Phi+2e^{2a}V(\Phi)\right]\right\}, \tag{2.23}$$

$$\partial_r\partial_r\Phi=\left[-\frac{g^2+1}{r}+2e^{4a}rg^2V(\Phi)\right]\partial_r\Phi - \frac{g^2}{N^2}\Phi+2g^2\left[e^{2a}\frac{dV(\Phi)}{d\Phi}-\alpha\nabla_\sigma\Phi\nabla^\sigma\varphi\right], \tag{2.24}$$

$$\partial_r(g^2)=g^2\left(\frac{g^2r}{N^2}T_{00}-\frac{g^2-1}{r}\right), \tag{2.25}$$

$$\partial_r(N^2)=N^2\left(rT_{11}+\frac{g^2-1}{r}\right), \tag{2.26}$$

where

$$T_{00}=\frac{N^2}{g^2}(\partial_r\varphi)^2+e^{2a}\left[\Phi^2+\frac{N^2}{g^2}(\partial_r\Phi)^2+2N^2e^{2a}V(\Phi)\right], \tag{2.27}$$

$$T_{11}=(\partial_r\varphi)^2+e^{2a}\left[(\partial_r\Phi)^2+\frac{g^2}{N^2}\Phi^2-2g^2e^{2a}V(\Phi)\right]. \tag{2.28}$$

The boundary conditions for this system of equations must take into account three things: (i) the solutions must be geometrically regular at the origin, (ii) the solutions must yield an asymptotically flat spacetime, and (iii) the solutions must take into account the cosmological input for both the coupling $a(\varphi)$ as well as φ.

Geometrical regularity at the origin means there is no conical singularity; i.e., the proper radius divided by the proper circumference should reduce to 2π at $r=0$. This implies that $g(0)=1$. Also, to maintain regularity in the field equations as $r\to 0$, we impose that $d\Phi/dr|_{r=0}=0$ and $d\varphi/dr|_{r=0}=0$.

For a purely technical reason to set $M_J=M_E$, we desire solutions that are asymptotically flat in both the Jordan and Einstein frames. That is, we want both $\tilde{g}_{\mu\nu}$ and $g_{\mu\nu}$ to reduce to the flat spacetime metric at spatial infinity. The implication of this is that the value of $\varphi_\infty\equiv\varphi(\infty)$ must be such that $a(\varphi_\infty)=0$. This is guaranteed since there is one more rescaling that has no analogue in GR. That is an invariance of the field equations if an arbitrary constant is added to the scalar-tensor coupling. If we simultaneously do the rescaling

$$e^c x\to x,\quad e^c\Phi\to\Phi,\quad e^c N\to N,\quad e^c\Lambda\to\Lambda \tag{2.29}$$

on the variables defined by Eq. (2.21) and let $a(\varphi)+c\to a(\varphi)$, then the field equations remain unchanged.

For the BD coupling, $\Phi_c\equiv\Phi(0)$ and φ_∞ are the only freely specified field values. The value of $N(0)$ is not specified freely, but rather is determined so that $\Phi(\infty)=0$. The value of φ at the origin is not specified freely; it must be determined in such a way that the solution for φ goes to φ_∞ at spatial infinity. We will use the freedom to add an arbitrary constant to the BD coupling $a(\varphi)$ so that all the solutions we consider have $\varphi_\infty=0$.

C. Evolution equations

We here assume that the gravitational scalar field is time dependent, $\varphi=\varphi(t,r)$, and use the rescaled bosonic field Ψ as $\Psi=\sqrt{4\pi G_*}\Phi$. Analogous to Eqs. (3.6)–(3.10) in [8], we introduce scalar field momenta Π_φ and Π_Ψ:

$$\Pi_\varphi=\frac{g}{N}\partial_t(r\varphi)\equiv\frac{1}{\beta}\partial_t(r\varphi), \tag{2.30}$$

$$\Pi_\Psi=\frac{g}{N}\partial_t(r\Psi)\equiv\frac{1}{\beta}\partial_t(r\Psi), \tag{2.31}$$

where we set $\beta=N/g$. The field equations become

$$\partial_t(r\varphi)=\beta\Pi_\varphi, \tag{2.32}$$

$$\partial_t\Pi_\varphi=(\partial_r\beta)\partial_r(r\varphi)+\beta\partial_r\partial_r(r\varphi)-(\partial_r\beta)(r\varphi)\frac{1}{r}-Ngr2\alpha e^{2a}\left[\frac{1}{2}\nabla_\sigma\Psi\nabla^\sigma\Psi^\dagger+2e^{2a}V(\Psi\Psi^\dagger)\right], \tag{2.33}$$

$$\partial_t(r\Psi)=\beta\Pi_\Psi, \tag{2.34}$$

$$\partial_t\Pi_\Psi=(\partial_r\beta)\partial_r(r\Psi)+\beta\partial_r\partial_r(r\Psi)-(\partial_r\beta)(r\Psi)\frac{1}{r}-2Ngr\left[e^{2a}\frac{dV(\Psi\Psi^\dagger)}{d\Psi^\dagger}-\alpha\nabla_\sigma\Psi\nabla^\sigma\varphi\right]. \tag{2.35}$$

Note that Ψ and Π_Ψ are complex variables, and so Eqs. (2.34) and (2.35) have two components. The momentum constraint and the G_{rr} component of the Einstein equations become

$$\partial_t g=N\left[\Pi_\varphi\partial_r\varphi+e^{2a}\frac{1}{2}(\Pi_\Psi^\dagger\partial_r\Psi+\Pi_\Psi\partial_r\Psi^\dagger)\right], \tag{2.36}$$

$$\partial_r N=\frac{N}{2r}(g^2-1)+\frac{Nr}{2}\left((\partial_r\varphi)^2+\Pi_\varphi^2\frac{1}{r^2}+e^{2a}\left[(\partial_r\Psi)(\partial_r\Psi^\dagger)+\Pi_\Psi\Pi_\Psi^\dagger\frac{1}{r^2}-2g^2e^{2a}V(\Psi\Psi^\dagger)\right]\right). \tag{2.37}$$

We use the above set of equations (2.32)–(2.37) for evolving the system and use the Hamiltonian constraint equation

$$2\frac{\partial_r g}{gr}+\frac{g^2-1}{r^2}=\frac{\Pi_\varphi^2}{r^2}+(\partial_r\varphi)^2+e^{2a}\left[\frac{\Pi_\Psi\Pi_\Psi^\dagger}{r^2}+(\partial_r\Psi)(\partial_r\Psi^\dagger)+2g^2e^{2a}V(\Psi\Psi^\dagger)\right] \tag{2.38}$$

to check the accuracy of our simulation.

D. Numerical techniques

1. Equilibrium configurations

We use a fourth-order Runge-Kutta algorithm to solve the differential equations (2.23)–(2.26). In order to find an equilibrium configuration, our system requires a two parameter search to find a solution that satisfies the boundary conditions for both Φ_∞ and φ_∞. Operationally, we choose a central value of the scalar field Φ_c first together with a guessed central value of the gravitational scalar field $\varphi(0)$, and inte-

grate out to large radii for different values of $N(0)$. We then check if the resulting φ_∞ is close to our expected boundary value.

The falling off behavior for the gravitational scalar field φ is much slower than the matter scalar field Φ. Therefore, at the numerical boundary, say, $r=r_{\rm end}$, we set the expected boundary value for $\varphi(r_{\rm end})$ as $\varphi(r_{\rm end})=\varphi_\infty+C/r_{\rm end}$, where a constant C is given by $C=-r_{\rm end}^2\, d\varphi(r)/dr|_{r=r_{\rm end}}$. If the computed $\varphi(r_{\rm end})$ is not the expected value, then we change $\varphi(0)$ and repeat the whole procedure. We set the tolerances to judge convergence in $\varphi(r_{\rm end})$ as 5×10^{-7}. More details are in [19].

2. Evolutions

We use the same code that was used in [8] for evolutions with modifications to incorporate BD theory. A polar-slicing condition [26] for the lapse is hard wired into the code. This slicing is highly singularity avoiding, and in the event of the formation of an apparent horizon, the lapse rapidly collapses and the radial metric blows up, crashing the code, indicating imminent black hole formation. The lapse equation (2.37) is integrated once on every time slice using a sixth-order integration scheme. The Hamiltonian constraint equation (2.38) is monitored as an indicator of the accuracy of the simulation and is not solved during the evolution. A leapfrog evolution scheme is used as described in [10].

For the boundary conditions regularity dictates that the radial metric be equal to 1 at the origin. The boson field and the BD field are both specified at the origin. The boson field goes to zero at ∞ and the BD field goes to a constant which is fixed during the evolution. This constant does not enter into any of the evolution equations as all the terms in the set of equations are derivatives in the BD field.

The inner boundary at the origin requires that the derivatives of all the metrics and fields vanish at this point. This is implemented by extending the range of r to include negative values. The metric components g, N, the boson field, and the BD field are required to be symmetric about $r=0$. The code itself uses new field variables which are the original fields times r for both the boson fields as well as the BD field and the momentum variables Π described in the previous section. Thus the code field variables as well as Π_φ and Π_Ψ are antisymmetric about $r=0$. The bosonic and BD fields at the origin during the evolution are determined from the first derivatives of the code fields there. For the radial metric the value at the boundary is determined from the Hamiltonian constraint equation (2.38).

In order to prevent reflections from the edge of the grid we use an *outgoing wave* condition at the outer edge of the grid (far away from the star) for the matter field Ψ and the BD field φ.

For the BD field φ, we impose the condition that the wave behave as

$$\varphi(r,t)=\varphi_\infty+\frac{1}{r}F\left(t-\frac{r}{c}\right), \tag{2.39}$$

which is a natural outgoing wave condition in spherically flat spacetime, and which is the proper assumption for the asymptotic region. Differentiating, one gets

$$\left.\frac{1}{c}\frac{\partial\varphi}{\partial t}+\frac{\partial\varphi}{\partial r}+\frac{(\varphi-\varphi_\infty)}{r}\right|_{\rm outer\ edge}=0. \tag{2.40}$$

Note that this is the same technique used by Novak [25], who studied a stellar collapse in scalar-tensor theory.

For the boson field Ψ, an asymptotic solution of the form $e^{-kr}e^{i\Omega t}/r$ to order $1/r$ is assumed. This gives an outgoing boundary condition to this order of

$$\beta^2k^2=\Omega^2-N^2m^2e^{2a}. \tag{2.41}$$

This dispersion relation is nontrivial for a massive scalar field. There is no perfect algorithm to implement it. At the outermost grid point we require that

$$\partial_t\partial_t\tilde{\Psi}=-\beta\partial_t\partial_r\tilde{\Psi}-\frac{N^2}{2}\,\tilde{\Psi}e^{2a}, \tag{2.42}$$

where $\tilde{\Psi}=r\Psi$. The second term on the right is a finite mass correction to leading order.

In addition to removing second-order reflections we substituted a sponge for the matter field (it reduces the momentum of the boson field artificially, and is irrelevant for the massless BD field) which is a potential term that is large for incoming waves (proportional to $k+\Omega$) and small for outgoing waves (proportional to $k-\Omega$). Therefore, we add an additional term in the evolution equation for Π_Ψ, Eq. (2.35),

$$\frac{V(\Psi\Psi^\dagger)}{e^aN}(\Pi_\Psi+\partial_r\tilde{\Psi}), \tag{2.43}$$

for $r_{\rm end}-D\leqslant r\leqslant r_{\rm end}$, where $r_{\rm end}$ is the r value of the outermost grid point and D is an adjustable parameter representing the width of the sponge. D is typically chosen to be a few times the wavelength of the scalar radiation moving out.

The code is tested with equilibrium configuration data (the zero-perturbation case). We confirm that the evolutions leave the metric and BD fields perfectly static for several thousand time steps. We also checked the code by taking a large number of BD parameters $\omega_{\rm BD}$ which would converge to the results in GR.

III. EQUILIBRIUM SEQUENCES

Before starting the dynamical study of boson stars, we describe briefly the equilibrium solutions in BD theory.

The existence of ground state boson stars in BD theory is reported in [17] for the case of $\omega_{\rm BD}=6$. The masses of the boson stars become smaller than the corresponding configurations in GR. They also show the effects of the interaction term Λ. In [19], the existence of higher node (excited) states is reported. They find that if the observational limit on $\omega_{\rm BD}$ is admitted, then the obtained configurations are very similar to GR. They also describe the stability of the ground state configurations using catastrophe theory. However, the whole discussion on the stability including the excited states is un-

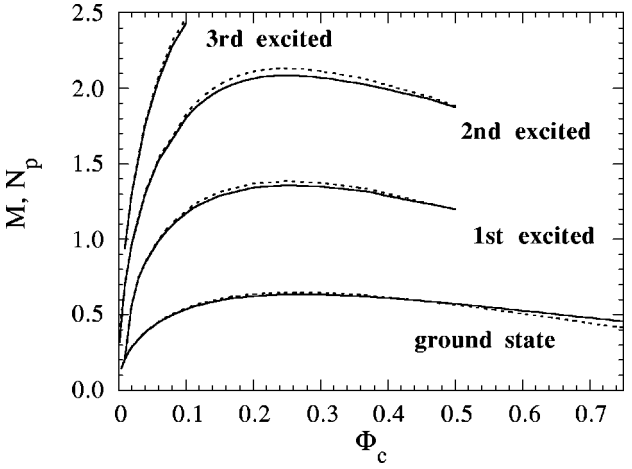

FIG. 1. Stable configurations of a boson star in Brans-Dicke theory. Masses of the ground state and excited state stars up to three nodes are shown as functions of the central matter field Φ_c. The solid lines and the dotted lines are the mass $M/(G_*/m)$ and the particle number $N_p/(G_*/m^2)$, respectively.

confirmed up to now. Also the dynamical behavior of this system is totally unknown.

In Fig. 1, we show the sequences of equilibrium configurations of boson stars in BD theory both for ground states and excited states up to three nodes. These sequences are given by solving the set of equations described in Sec. II B, and we applied the BD parameter $\omega_{\rm BD}=600$ for plotting this figure. The total mass of the boson star, M, and its particle number N_p (in units of m) versus the central boson density Φ_c profile is plotted. We see that, in the ground and excited state sequences, the signature of the binding energy $M-mN_p$ goes from negative to positive according to the value of Φ_c. Configurations with positive binding energy are expected to be dispersive.

In the case of GR, we know the star ground state configurations to the left of the central maximum are *stable*. By ''stable,'' we mean that under perturbations they move to new configurations on the same branch (left of the maximum). We naturally suspect that the branch to the left of the maximum in the BD profile is also stable. Therefore, in this and all further sections of this paper, we will refer to ground state boson star configurations to the left of the maximum mass in Fig. 1 as the *S*-branch configurations and others as *U*-branch configurations. From the catastrophe discussion [19], we also suspect that the *U*-branch configurations are unstable.

The boson star system exhibits anisotropies due to the presence of scalar fields. Here, ''anisotropy'' means the difference of the radial pressure from the tangential pressure in these configurations $[|T^r_r|\neq|T^\theta_\theta|$, where T^ν_μ is the energy-momentum tensor defined as the right-hand side of Eq. (2.9)]. In the case of a scalar-tensor theory this anisotropy could change from GR due to the presence of the additional gravitational scalar field. In the case of BD theory, we find the anisotropy slightly but not significantly lower as compared to GR. In Fig. 2, we show the fractional anisotropy

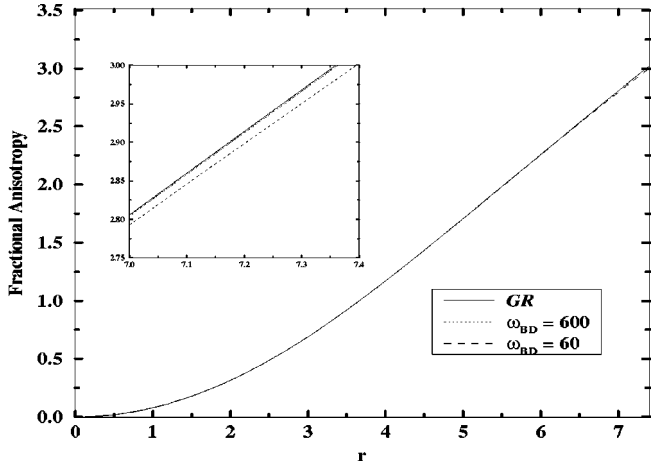

FIG. 2. Fractional anisotropy (3.1) is plotted for ground state configurations of central boson density $\Phi_c=0.2$ for GR and BD theory ($\omega_{\rm BD}=600$ and 60). The inset is the magnification of the range $r=7.0-7.4$.

$$f_a=(T^r_r-T^\theta_\theta)/T^r_r \tag{3.1}$$

for a ground state boson star with $\Phi_c=0.2$ for GR and BD theory with $\omega_{\rm BD}=600$ and 60. In Fig. 3, we show the fractional anisotropy for three nodes' (third excited) states of boson stars in BD theory, $\omega_{\rm BD}=600$, with different Φ_c. At the nodes where the boson field derivative vanishes, all those fractional anisotropies are close to 2, which is the analytically expected number. This is because we can write the equilibrium fractional anisotropy as

$$\frac{2[(\partial_r\varphi)^2+e^{2a}(\partial_r\Phi)^2]}{(\partial_r\varphi)^2+e^{2a}\left[(\partial_r\Phi)^2+(g^2/N^2)\Phi^2-2g^2e^{2a}V(\Phi)\right]}. \tag{3.2}$$

At the nodes, $\Phi=0$, and as a result, $V(\Phi)$ also vanishes.

The plots end at the radius of the boson star (we define the radius to be the 95% mass radius of these systems). Consis-

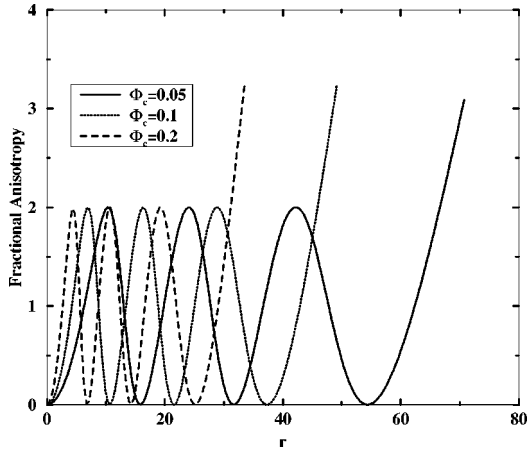

FIG. 3. Fractional anisotropy (3.1) is plotted for three-node (third excited) states in BD theory ($\omega_{\rm BD}=600$) with different central boson densities $\Phi_c=0.05$, 0.1, and 0.2. The plots end at the radius of each star (95% of the total mass).

tent with Gleiser's results in the GR case [28], we have seen that the fractional anisotropy at the radius of the stars is almost the same number for all configurations. One of the consequences of these anisotropies is that we cannot apply the adiabatic perturbation method to discuss the stability of this system, as discussed by Kaup [1].

IV. STABILITY OF GROUND STATE EQUILIBRIUM STATES

In order to confirm whether the stars on the *S* branch of the ground state in Fig. 1 are stable, we show our simulation of the perturbed configurations of the *S*-branch stars in this section.

Our perturbations themselves simulate the annihilation (creation) of particles by enhancing (reducing) the boson field smoothly in some region of the star. A typical perturbation is put in for a region of the star from r_1 to r_2 and is of the form

$$\Phi_{\text{perturbed}}(r)=\Phi_{\text{original}}(r)\left\{1+p\ \sin^n\left(\pi\frac{r_2-r}{r_2-r_1}\right)\right\}, \tag{4.1}$$

where p is the perturbation size and is positive for particle creation and negative for annihilation, and n is an integer that can be varied.

This perturbation is put in at the initial time step and the lapse equation and Hamiltonian equation are reintegrated to give new metrics for this scalar field and original BD field. The momentum associated with the BD field is set to be *zero* on the initial time slice.

A. Small perturbation of bosonic scalar field

After we confirmed that our code retains its equilibrium profile for long time evolutions, we start our evolutions of an *S*-branch equilibrium state with a tiny perturbation. Here, ''tiny'' means that the difference of the mass between the original and new configuration is less than 0.1%. We find that the system begins oscillating with a specific fundamental frequency, called a quasinormal mode (QNM) frequency. Figure 4 shows the oscillations of the metric and the BD field for a boson star of central boson field density $\Phi_c=0.2$ and with $\omega_{\text{BD}}=600$. We see the BD field, as well as the metric function, start oscillating at the same frequency. A Fourier transform of the metric and BD field data shows the overall frequency of the star to be $(2/\pi)0.03$ in nondimensional units. This is quite close to the case in GR.

In GR, a QNM frequency increases as Φ_c become larger (radius becomes smaller) up to a point before starting to decrease rapidly to zero as it approaches the density corresponding to maximum mass, signalling the onset of instability [8]. We found the same feature in BD theory.

In addition, the system takes on the proper underlying frequency, which originates from the time dependence of the boson field $\Psi\sim e^{it}$. This frequency corresponds to a 2π period in t in our units, and appears in the metric and BD field oscillation with a π period, from the structure of the equations. To show this feature we have enhanced the BD field oscillation (Fig. 4) in Fig. 5. The time interval between the ticks on the horizontal axis is π.

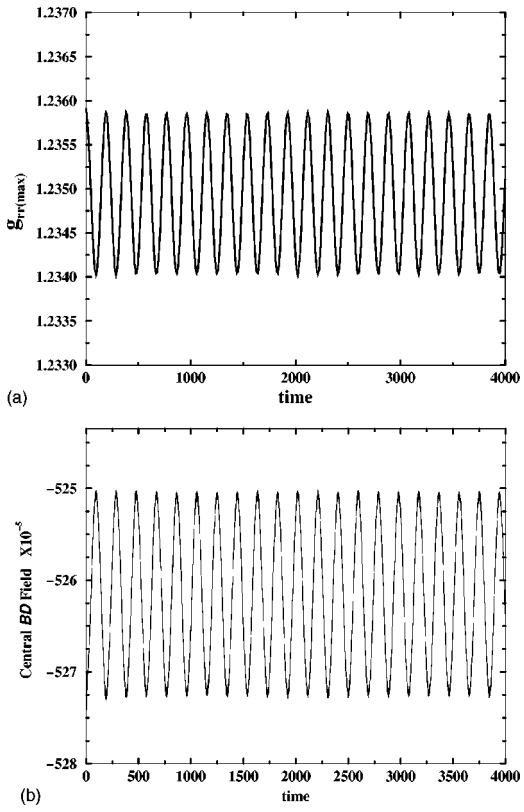

FIG. 4. Quasinormal mode oscillation of a stable boson star. The maximum value of the metric g_{rr} and the central Brans-Dicke field $\varphi(r=0)$ are plotted as functions of time. Both of them take on the QNM frequency of the star. The oscillation is virtually undamped for a long period of time.

B. Large perturbation of the bosonic scalar field

Under large perturbations, a stable boson star in GR expands and contracts, losing its mass at each expansion. The oscillations damp out in time and the system finally settles down into a new configuration on the *S* branch. These features are now observed in BD theory.

We show the effects of a large perturbation on a stable BD boson star described above. The example we present is the case of initial data with $\Phi_c=0.2$, mass $M=0.540G_*/m$ after perturbation (about 13% lower in mass compared to an unperturbed equilibrium configuration of $M=0.622G_*/m$).

The maximum radial metric g_{rr} and the central BD field as a function of time are shown in Figs. 6 and 7, respectively. In both figures, we plotted the case of $\omega_{\text{BD}}=600,60$ as well as GR. The increase of the maximum g_{rr} indicates that the star is contracting, reaching its maximum value at the end of the contraction in a cycle. Then, as the star expands, the maximum g_{rr} decreases, reaching its minimum at the end of the expansion. These processes repeat themselves with the oscillations damping out in time as the star settles to a new stable configuration with the maximum radial metric of a smaller value than it started with (lower mass). The lower

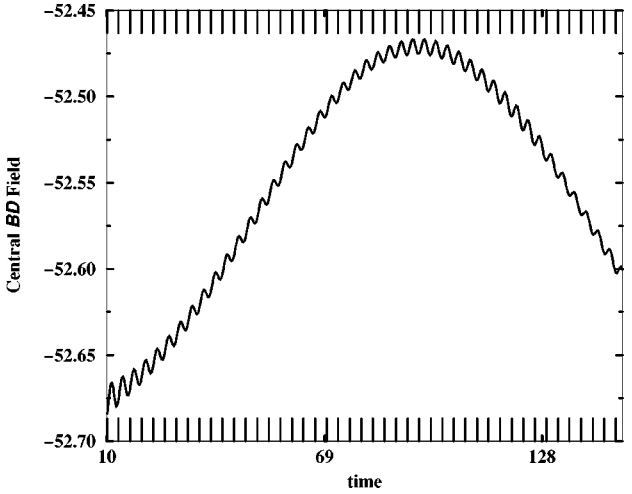

FIG. 5. The magnification of the second figure of Fig. 4. The time interval between the ticks on the horizontal axis is π. We see that the Brans-Dicke field has the underlying π oscillation that it takes on.

value of the BD parameter shows a phase shift in comparison to GR which might be suggestive of a different rate of approach to the final configuration. We see the same dynamical behavior in the BD field (Fig. 7). It has the same oscillation frequency as that of the metric. The oscillations damp out in time and the BD field settles to a value closer to zero than it started at (lower final mass).

The system loses mass through radiation during its evolution. A comparison of the mass as a function of time for the BD case ($\omega_{\rm BD}=600$ and 60) as well as GR shows little difference, indicating that the radiation is mostly scalar field radiation and not scalar gravitational radiation. This is despite the BD field oscillating in the BD case and being zero in the GR case.

The amount of mass radiated progressively decreases as can be seen in the luminosity profile ($-dM/dt$ versus time) shown in Fig. 8. Here again a comparison between GR and

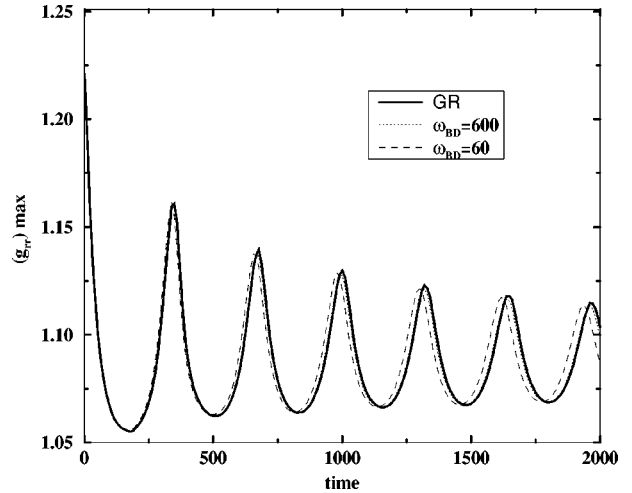

FIG. 6. Finite perturbation of an S-branch boson star. The maximum metric g_{rr} is plotted. The metric is damped in time as the star settles to a new configuration.

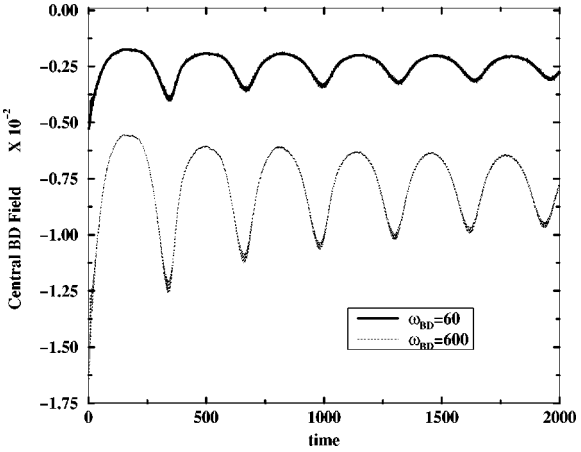

FIG. 7. The same model as Fig. 6. The central Brans-Dicke field $\varphi(r=0)$ is plotted. We see that the oscillations damp out as the star settles, indicating again a transition to a new stable boson star configuration.

the two BD parameters is shown. Again we see the phase shift for the lower BD parameter (further from GR). The system finally settles to a new state of smaller mass.

We have also conducted tests with perturbations that enhance the mass. For stable branch stars as in the case of GR [8] the star loses mass and settles to a new configuration on the same branch.

V. EVOLUTION OF *U*-BRANCH STARS AND EXCITED STARS

Boson stars on the U branch and excited states are inherently unstable in GR [10]. Under perturbations that reduce the mass, boson stars on the U branch can migrate to the stable branch. In this section, we will see these features in BD theory too. They can be perturbed in a way so as to decrease their mass enough that they migrate to new configurations on the S branch. On the other hand, in GR, if they do not lose mass and migrate, then the boson stars of configurations with $M<N_p m$ collapse to black holes. Stars with

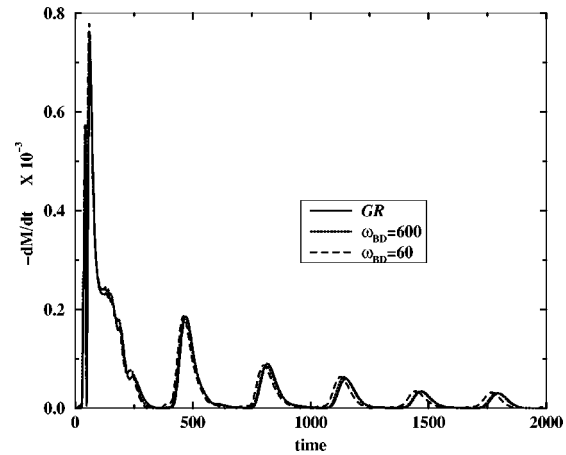

FIG. 8. The same model as the previous figures. The ''luminosity'' $L=-dM/dt$ is plotted versus time. Clearly the radiation is decreasing in time.

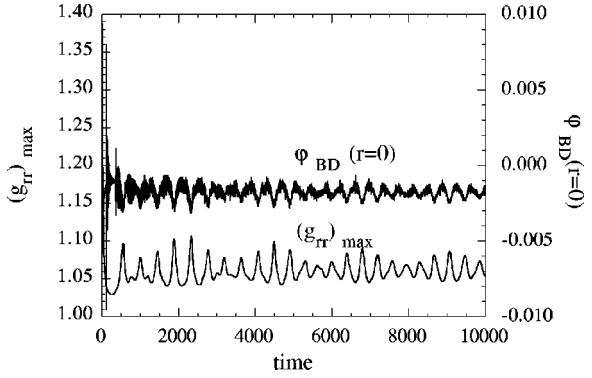

FIG. 9. Migration of an unstable boson star to a stable configuration; the central Brans-Dicke field $\varphi(r=0)$ and maximum of g_{rr} are plotted. There is a sharp initial drop in the radial metric as the star moves to the stable branch. The oscillations damp out in time as the star settles.

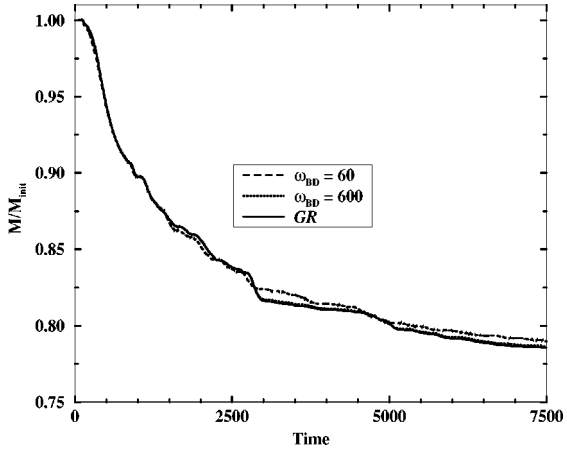

FIG. 10. Comparisons of the total mass of the system M rescaled by its initial mass $M_{\rm init}$ during a migration process from a U-branch star. Three lines are plotted. Although the mass loss is similar in the three cases, the higher Brans-Dicke case clearly is closer to GR as it should be.

$M > N_p m$ are dispersive and radiate out to infinity. We will see also these features in BD theory.

A. Migration to a stable configuration

Our first dynamical example from U-branch boson stars is a migration process. As in GR, we have also seen migrations of these stars to the stable branch when we remove enough scalar field smoothly from some region of the star so as to decrease the mass by about 10%. In particular, we show the migration of a star of the central boson field $\Phi_c = 0.35$ with unperturbed mass $0.625 G_*/m$. After perturbation, its mass is reduced to $0.558 G_*/m$. In Fig. 9, we show the maximum value of metric g_{rr} and central value of the BD field $\varphi(r=0)$ versus time. The initial sharp drops in both lines occur as the star rapidly expands and moves to the stable branch. After that it oscillates and finds a new configuration to settle into. The damping of oscillations as it settles is clearly seen in the figure. We see also the BD field oscillations damping out as the star gets closer and closer to its final state.

The ratio of mass at time t to the initial mass for BD theory with parameter $\omega_{\rm BD} = 60$, 600 and the GR case is shown in Fig. 10. The flattening of the curve at later time is indicative of the star settling down to a new configuration. Although convergence towards GR with increasing $\omega_{\rm BD}$ is clearly indicated, there is no significant difference between the three cases. The amount of the total mass extraction from the system is slightly suppressed if we evolve in BD theory. By the time of 7500 shown in the plot, we see that the mass of the star is about $0.045 G_*/m$, which corresponds to an equilibrium configuration with $\Phi_c = 0.06$, while our central density Φ_c is about 0.061, meaning that the star is quite close to its final configuration.

B. Transition to black hole

Contrary to the previous example, if we add a small mass to U-branch stars, we can see the formation of a black hole in its evolution. In Fig. 11, we plotted an example of such evolution, which indicates the formation of a black hole. The initial datum of this plot is the boson star of the central boson field $\Phi_c = 0.35$, which is the same value as the previous migration case with an unperturbed mass of $0.625 G_*/m$. The system is perturbed very slightly so that the perturbed initial mass is $0.628 G_*/m$, which is less than 0.5% greater than its initial mass. This is less than the maximum mass of a boson star of $0.632 G_*/m$ in the sequence of $\omega_{\rm BD} = 600$. The sudden collapse of the lapse function is indicative of the imminent formation of an apparent horizon due to the polar-slicing condition in our code [26]. In addition to this the radial metric starts to blow up and the code is no longer capable of dealing with the sharp gradients and crashes. As an indicator of the suddenness of the process, we see that in the configuration shown the lapse has fallen to a value of about 0.003 by a time of 60 after being at 0.230 at a time of 55 and 0.5 at a time of 50 (the latter two points are not

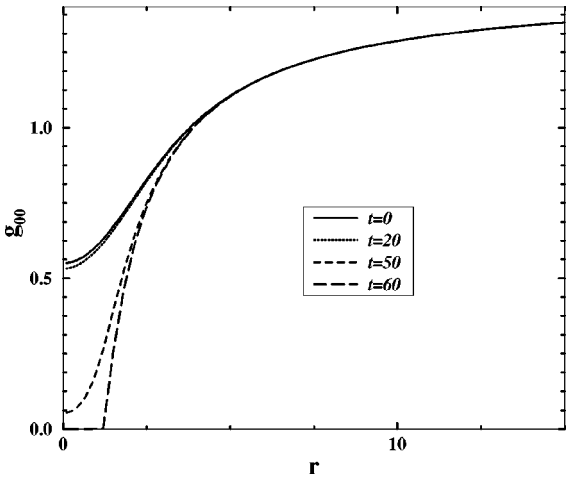

FIG. 11. Dynamical transition from a U-branch star to a black hole. The metric g_{00} is plotted. The collapse of the lapse function is indicative of imminent black hole formation.

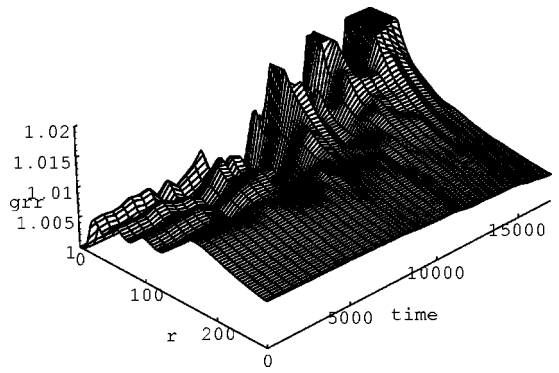

FIG. 12. Dynamical transition from an excited state to a ground state boson star configuration. The metric g_{rr} is plotted. The initial four peaks indicative of a three-node star cascades to the ground state after a long time evolution.

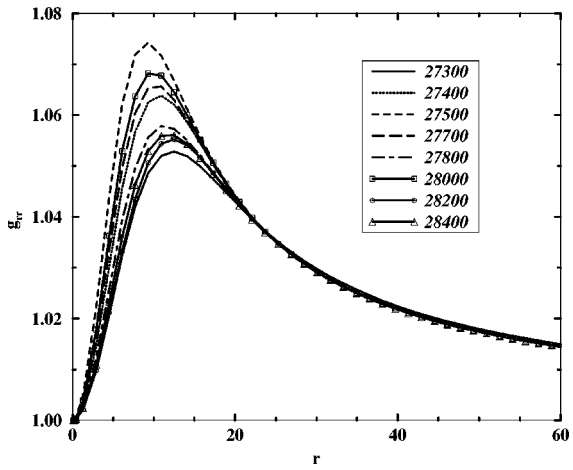

FIG. 13. Dynamical transition from an excited state to a ground state boson star configuration. The metric g_{rr} is plotted at later times to show its oscillations after the star reaches a ground state.

shown in the plot). The lapse value at the edge of the grid is greater than 1 because it has been scaled by the underlying frequency of the system Ω.

There is almost no loss in mass in this system and the time of collapse is quite similar to GR. In the GR case, we confirmed the formation of a black hole [29] very shortly after this point ($\approx 3M$ where M is the mass of the system) by switching this data into a three-dimensional code and evolving the system. Therefore we expect almost the same behavior in the BD case.

Note that we have seen this behavior for denser boson stars with lower masses and the same order of perturbation. This is true as long as they have $M<Nm$.

Black hole formation in BD theory is investigated by Scheel, Shapiro, and Teukolsky for the dust collapse case [23]. They found that the dynamical behavior of horizons (both event horizon and apparent horizon) is quite different in the physical Brans-Dicke frame, but the same as GR in the Einstein frame. Their results therefore also support our discussion of the formation of black hole in BD theory.

We cannot show the emitted scalar waveform because we are using the polar-slicing condition and cannot proceed with the evolution after the collapse of the lapse. We are planning to evolve this system after the formation of a black hole in a three-dimensional code. The results will be reported in the future.

C. Transition to the ground state from the excited state

Excited states of boson stars in general are not stable in the GR case. They form black holes if they cannot lose enough mass to go to the ground state. We confirm the same features for the BD case. In Fig. 12, we plot the metric g_{rr} of the dynamical transition from an excited state with three nodes to a ground state boson star configuration. This star had an unperturbed mass of $3.249G_*/m$, corresponding to a central density $\Phi_c=0.01$. After perturbation its mass was reduced to $0.919G_*/m$. The initial configuration has four metric maxima and the final has one showing the transition. After it goes to the ground state, it oscillates and compactifies to form a new configuration. We show the oscillations of the star from a time of 27 300 to 28 400 in Fig. 13. The 95% mass radius at this stage is about 100 and the star has still to continue its evolution for a while longer. The amount of mass loss in this process is quite similar to the migration case (cf. Fig. 10). We also found that the difference of the theory is little.

Any configuration of an excited state star with a mass less than the maximum mass of a ground state star is expected to go to the ground state. However, since higher excited state S-branch configurations have progressively greater masses for the same central density (mass of n nodes$>n-1>\cdots>1>$ground state boson stars), the configurations with masses less than the maximum ground state mass get more and more dilute. We have seen the tendency of these stars to migrate to the ground state in our tests. In [10], such cases have been described for the GR case. Since these dilute configurations correspond to large stars with low oscillation frequencies, to evolve them until they go to the ground state is numerically very costly as they take a very long time to do so. Configurations with slightly larger masses may also be able to lose enough mass during their evolution and transit to the ground state. An exact parameter search though would be very time consuming. We have rather chosen to just exemplify the possibility of transitions with our example. We have taken a denser configuration to reduce the time scale of evolutions and then perturbed it so much to ensure that no black hole forms. In fact we can just think of the system as a perturbed distribution of bosonic fields that has three nodes and which transits to the ground state rather than compare the perturbed system to the original unperturbed one.

VI. FORMATION OF BOSON STARS IN BRANS-DICKE THEORY

In the previous sections, we analyzed boson stars in BD theory, starting with those equilibrium or perturbed equilibrium configurations. However, we have not discussed whether or how such an equilibrium configuration actually forms in BD theory. In this section, we answer this question

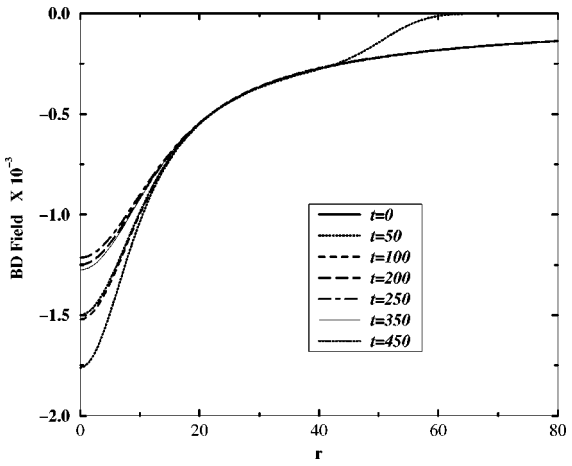

FIG. 14. An example of the formation of a boson star in Brans-Dicke theory. Snapshots of $\varphi_{\rm BD}(r)$ are plotted for the initial stage of evolution.

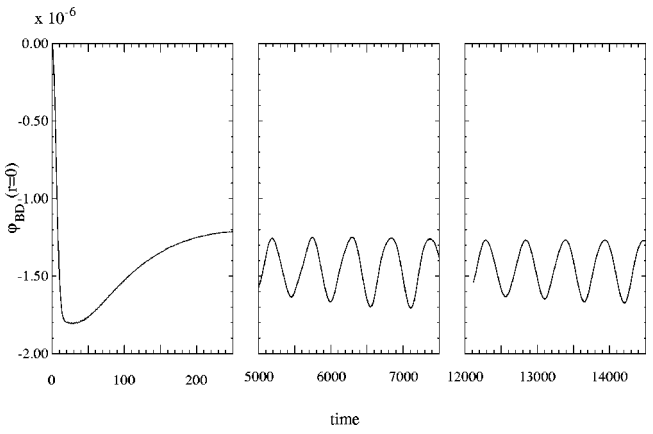

FIG. 15. An example of the formation of a boson star in Brans-Dicke theory. The dynamical behavior of the Brans-Dicke scalar field $\varphi_{\rm BD}(x=0)$ is plotted for three evolution regions: earlier time, middle time, and later time. We can see the field settling down to an equilibrium configuration (periodic oscillation).

by demonstrating the formation of boson stars in BD theory. The formation of boson stars in GR has been discussed by Seidel and Suen [30].

We start our evolution with the initial data that have a Gaussian packet in the bosonic field Φ, which represents a local accumulation of the matter field:

$$\Phi = a\ \exp(-bx^2), \tag{6.1}$$

where a and b are free parameters. We set the BD field φ to be flat at the initial stage, so as to see if local inhomogeneity of the matter will form a boson star in BD theory. We integrate the lapse equation (2.36) and Hamiltonian constraint equation (2.38) to provide metric functions on the initial slice. We then evolve the set of dynamical equations (2.32)–(2.35).

We find that, with the particular parameters a and b, this system actually forms a stable, equilibrium configuration, which might be recognized as the formation of a boson star. As a demonstration, we show here an evolution with parameters $a=0.1$ and $b=0.025$. The BD parameter $\omega_{\rm BD}$ is taken to be 600. In Fig. 14, we show the BD field φ as a function of radial coordinates at various earlier times of evolution. We see that the BD field becomes negative quickly and begins oscillating around a particular value. Actually the reader will find that the BD field φ is jumping around $r=40-50$ at $t=50$. The long time evolution of the BD field is shown in Fig. 15, in which we show the BD scalar field $\varphi_{\rm BD}$ at the center for earlier times, middle times, and later times. We can see the field settling down to a periodic oscillation in the final phase, like in the migration and transition cases in the previous section. The initial mass of this configuration in units of G_* is 0.39 and the final (at the end of our simulation) about 0.384. At this stage the magnitude of the central boson field is oscillating between 0.032 and 0.048. The BD field oscillates between -0.00126 and -0.00166. This range of boson oscillations corresponds to masses between 0.342 and 0.410, respectively, while the BD field oscillations give a mass between 0.355 and 0.405, respectively. Given that the mass at this stage is 0.384 (consistent with the above) we expect that the final mass will be between 0.355 and 0.384.

We show the luminosity $L(=-dM/dt)$ versus time t curve in Fig. 16 within the same periods as in Fig. 15. In the early stage, we see that one pulse is emitted from the system. This is related to the outgoing pulse from our initial boson field setting. After this initial pulse the system slowly takes on the characteristic π oscillation of $|\Psi|^2$ of the star as the star begins forming. After that, we see that L begins damped oscillations versus t. (We cut out the initial large amplitude luminosity around $t=200$.) The system's evolution is followed for a long time: however, the accuracy of the calculation is quite good with the Hamiltonian constraint satisfied to order 10^{-7} or better.

We also note that certain parameters a and b (mentioned at the beginning of this section) will result in the formation

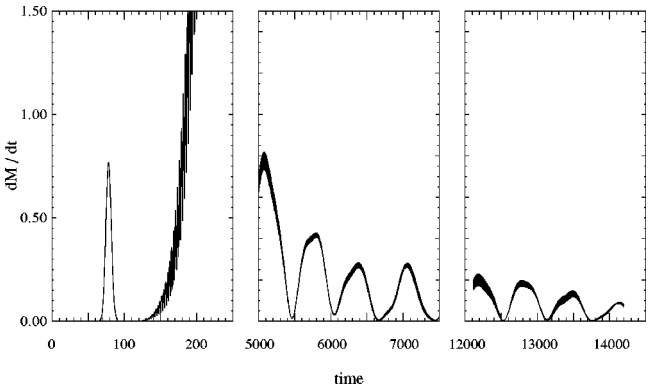

FIG. 16. Similar to Fig. 15, the emitted luminosity $L=-dM/dt$ is plotted. In the first evolution stage, the luminosity data take on the underlying boson field square oscillation, after having emitted one scalar pulse, related to the initial field configuration: Gaussian pulse. The amount of mass loss decreases in time as the formed star settles.

but others will not. If we choose a large amplitude a and small b, then the initial configuration has too large a mass and is not dispersive enough, resulting in black hole formation during evolution. In the opposite limit, if we have a very narrow localized wave packet, it has a tendency to be dispersive, since it has more momentum from the classical analogue of the uncertainty principle. So, if b is too large, no boson star forms. Intermediate between these two are configurations that form stable stars. For example, if $a=0.1$, $b=0.01$, a black hole is formed; $b=0.025$ results in boson star formation as we have shown, and $b=0.035$ becomes flat space at the end of the evolution. On the other hand, for $b=0.01$ and $a=0.05$ a boson star forms.

VII. CONCLUDING REMARKS

We studied the dynamical features of boson stars in the Jordan-Brans-Dicke (BD) theory of gravity. By evolving the system numerically, we discussed the stability of those ground state S-branch equilibrium configurations, black hole formation, and migration from a U-branch solution, and transition processes from excited state to ground state, together with those scalar wave emissions (mass loss from the system).

We showed that the basic features are the same as the general relativity (GR) cases [10]. Since we choose the BD parameter $\omega_{\rm BD}=600$ for most simulations, as we are interested in those observationable differences with GR, the signatures of boson stars such as the oscillation frequency of the final S-branch configurations and the emitted waves' luminosity are quite identical with GR. The scalar wave emissions are slightly suppressed than in GR. These results indicate to us that the scalar modes of gravity in the boson star system are already dominated by the boson scalar field; thus an additional gravitational scalar field does not change the dynamical behavior in the BD theory of gravity.

We also demonstrated the formation of a boson star from a Gaussian packet of a bosonic field and flat BD field. This success suggests to us that the boson star is a realizable object even in BD theory, and opens windows to study them in astrophysical roles including similar nontopological solitonic objects.

By showing that the U branch of ground state equilibrium is unstable, we have confirmed the stability discussions by Comer and Shinkai [19] for the BD ground state using catastrophe theory. Our next problem is to check their prediction in scalar-tensor theory, especially the Damour-Nordtvedt attractor model [20], with which they predict that boson stars in the early universe will not be formed. We are also now studying the existence of ''oscillations'' [31], self-gravitating solitonic objects made from a real scalar field, in scalar-tensor theory. These results will be reported elsewhere.

ACKNOWLEDGMENTS

We thank Ed Seidel and Wai-Mo Suen for letting us modify their general relativity boson star code [8] to scalar-tensor gravity. We also thank Greg Comer and Clifford Will for useful conversations. We again appreciate Wai-Mo Suen and Greg Comer for useful comments on our drafts. This work was partially supported by Grant Nos. NSF PHYS 96-00507, 96-00049, and NASA NCCS 5-153.

[1] D. J. Kaup, Phys. Rev. **172**, 1331 (1968).
[2] R. Ruffini and S. Bonazzola, Phys. Rev. **187**, 1767 (1969).
[3] R. Liddle and M. S. Madsen, Int. J. Mod. Phys. D **1**, 101 (1992).
[4] J. Balakrishna, E. Seidel, and W-M. Suen (in preparation).
[5] M. Colpi, S. L. Shapiro, and I. Wasserman, Phys. Rev. Lett. **57**, 2485 (1986).
[6] J. A. Frieman, G. B. Gelmini, M. Gleiser, and E. W. Kolb, Phys. Rev. Lett. **60**, 2101 (1988).
[7] T. D. Lee and Y. Pang, Nucl. Phys. **B315**, 477 (1989).
[8] E. Seidel and W-M. Suen, Phys. Rev. D **42**, 384 (1990).
[9] F. V. Kusmartsev, E. W. Mielke, and F. E. Schunck, Phys. Rev. D **43**, 3895 (1991); Phys. Lett. A **157**, 465 (1991); F. V. Kusmartsev and F. E. Schunck, Physica B **178**, 24 (1992).
[10] J. Balakrishna, E. Seidel, and W-M. Suen, gr-qc/9712064.
[11] C. H. Brans and R. H. Dicke, Phys. Rev. **124**, 925 (1961).
[12] C. M. Will, *Theory and Experiment in Gravitational Physics*, 2nd ed. (Cambridge University Press, Cambridge, England, 1993).
[13] R. D. Reasenberg, I. I. Shapiro, P. E. MacNeil, R. B. Goldstein, J. C. Breidenthal, J. P. Brenkle, D. L. Cain, T. M. Kaufman, T. A. Komarek, and A. I. Zygielbaum, Astrophys. J. **234**, L219 (1979).
[14] R. N. Treuhaft and S. T. Lowe, Astrophys. J. **102**, 1879 (1991).
[15] M. Saijo, H. Shinkai, and K. Maeda, Phys. Rev. D **56**, 785 (1997).
[16] D. I. Santiago, D. Kallingas, and R. V. Wagoner, Phys. Rev. D **56**, 7627 (1997).
[17] M. A. Gunderson and L. G. Jensen, Phys. Rev. D **48**, 5628 (1993).
[18] D. F. Torres, Phys. Rev. D **56**, 3478 (1997). The mistaken definition of mass is noted in his later paper, D. F. Torres, A. R. Liddle, and F. E. Schunck, *ibid.* **57**, 4821 (1998).
[19] G. L. Comer and H. Shinkai, Class. Quantum Grav. **15**, 669 (1998).
[20] T. Damour and K. Nordtvedt, Phys. Rev. Lett. **70**, 2217 (1993); Phys. Rev. D **48**, 3436 (1993).
[21] T. Matsuda and H. Nariai, Prog. Theor. Phys. **49**, 1195 (1973).
[22] M. Shibata, K. Nakao, and T. Nakamura, Phys. Rev. D **50**, 7304 (1994).
[23] M. A. Scheel, S. L. Shapiro, and S. A. Teukolsky, Phys. Rev. D **51**, 4208 (1995); **51**, 4236 (1995).
[24] T. Harada, T. Chiba, K. Nakao, and T. Nakamura, Phys. Rev. D **55**, 2024 (1997).

[25] J. Novak, Phys. Rev. D **57**, 4789 (1998).
[26] J. M. Bardeen and T. Piran, Phys. Rep. **96**, 205 (1983).
[27] R. Friedberg, T. D. Lee, and Y. Pang, Phys. Rev. D **35**, 3640 (1987); **35**, 3658 (1987).
[28] M. Gleiser, Phys. Rev. D **38**, 2376 (1988); **39**, 1257(E) (1989).
[29] J. Balakrishna, G. Daues, E. Seidel, and W-M. Suen (in preparation).
[30] E. Seidel and W-M. Suen, Phys. Rev. Lett. **72**, 2516 (1994).
[31] E. Seidel and W-M. Suen, Phys. Rev. Lett. **66**, 1659 (1991).
[32] J. Balakrishna, G. L. Comer, and H. Shinkai (in preparation).